Laser and Particle Beams (1989), *vol.* 7, *part* 3, *pp.* 551–559
Printed in Northern Ireland

RF production of high density plasmas for accelerators

By FRANCIS F. CHEN
Electrical Engineering Department, University of California, Los Angeles, California 90024, U.S.A.

(Received 24 September 1988)

Preliminary experimental results are shown on the production of plasmas by low frequency helicon waves. At constant rf frequency and power, the results show a maximum in density as the dc magnetic field is varied. The measurements confirm the theoretical expectation that the plasma is ionized by Landau damping of the radiofrequency waves.

1. Introduction

In recent years many ideas have emerged on new ways to use dense plasmas to improve the performance of high-energy particle accelerators (Chen 1989). Devices such as the beat-wave accelerator, the wake field accelerator, and the plasma lens for final focus all require plasmas in the density range 10^{14}–10^{18} cm^{-3} with dimensions of the order of millimeters in diameter and tens of centimeters in length. Furthermore, the plasmas must satisfy a number of requirements. They must be quiescent and uniform, or have controllable density profiles, in both the radial and longitudinal directions. The density must be maintained in steady state or be reproducible in short pulses to within a few percent. This usually means that the atoms should be fully stripped to avoid ionization by the laser or particle beam. There should be access for these beams along the axis. Finally, the confining magnetic field, if any, should not perturb the trajectories of the beam particles in an uncontrollable manner. Up to now, the following plasma production methods have been used in laser-plasma experiments, but none of them satisfies all of the criteria above: (1) high current arc, (2) theta pinch, (3) z-pinch, (4) laser ionization of gas puffs, (5) laser ionization of thin foils, (6) multi-photon ionization with high-power lasers, and (7) ultraviolet ionization. In this paper, we explore the possibility of using a helicon wave source for these purposes.

Fully ionized plasmas in the 10^{12}–10^{13} cm^{-3} range using only 1 kW of rf power and a 1-kG field have been reported by Boswell *et al.* (1982) and Boswell (1984). The unusually high efficiency has been explained in terms of Landau damping by Chen (1985). Helicons are low-frequency whistler waves ($\omega \ll \omega_c$) in which the main current is carried by the $E \times B$ motion of the electrons. The waves are partly electromagnetic and partly electrostatic. Ion motions can be neglected at frequencies well above the lower hybrid frequency. Because of the low frequency, the parallel phase velocity ω/k_z can be made low enough to match the thermal velocity of the electrons, thus giving rise to efficient transfer of energy from the wave to the main body of the electron distribution via Landau damping.

2. Summary of theory

From the governing equations

$$\nabla \times E = -\partial B/\partial t, \quad \nabla \times B = \mu_0 j, \quad \nabla \cdot B = 0, \tag{1}$$

$$E_\perp = j \times B_0/en_0, \quad E_z = \eta j_z, \tag{2}$$

0263-0364/89/0703-0551$05.00

one easily finds that perturbations of the form $B\exp[i(m\theta + kz - \omega t)]$ in the $\eta = 0$ limit follow

$$j_1 = (\alpha/\mu_0)B_1 \tag{3}$$

$$\nabla^2 B_1 + \alpha^2 B_1 = 0, \tag{4}$$

where

$$\alpha = (\omega/k)(\mu_0 e n_0/B_0). \tag{5}$$

Equation (4) can be solved in cylindrical coordinates, and the result is most easily expressed in terms of the right- and left-hand circularly polarized components B_R, E_R, B_L, and E_L:

$$B_R = A(\alpha + k)J_{m-1}(\mathrm{Tr}) = -i(k/\omega)E_R \tag{6}$$

$$B_L = A(\alpha - k)J_{m+1}(\mathrm{Tr}) = i(k/\omega)E_L \tag{7}$$

$$B_z = -i\sqrt{2}ATJ_m(\mathrm{Tr}), \quad E_z = 0. \tag{8}$$

Here J_m is a Bessel function of the first kind, and T is a transverse wavenumber defined by

$$T^2 = \alpha^2 - k^2. \tag{9}$$

Both insulating and conducting boundary conditions at $r = a$ lead to the condition

$$m\alpha J_m(\mathrm{Ta}) = TkaJ'_m(\mathrm{Ta}) = 0, \tag{10}$$

where $(')$ is the derivative of J_m with respect to its argument. In particular the lowest two modes satisfy

$$J_1(\mathrm{Ta}) = 0 \qquad (m = 0) \tag{11}$$

$$J_1(\mathrm{Ta}) = (Tka/2\alpha)(J_2 - J_0) \simeq 0 \quad (m = 1). \tag{12}$$

The dispersion relation is given by equations (5, 9, and 10).

The case of finite resistivity η can be treated by perturbing the previous solution. The parallel current j_z then requires a component $E_z = \eta j_z$ to drive it, and for real ω there is a complex k and a damping length $L_c = 1/\mathrm{Im}\,(k)$. In the collisionless case, electron motion along B_0 is controlled by the Vlasov equation, and one obtains an effective resistivity η_{eff} due to Landau damping:

$$1/\eta_{\mathrm{eff}} = i\omega\varepsilon_0(\omega_p^2/\omega^2)\zeta^2 Z'(\zeta), \tag{13}$$

where $\zeta = \omega/kv_{\mathrm{th}}$ and $Z'(\zeta)$ is the derivative of the plasma dispersion function (Chen 1984). Expressing η in terms of the electron-ion collision frequency $\nu_{ei} = n_0 e^2\eta/m$ and using the asymptotic expansion for $Z'(\zeta)$, we obtain the damping lengths

$$L_c = (1/k)(\omega_p^2/c^2T^2)(\omega/\nu_{ei}) \tag{14}$$

$$L_{LD} = (1/k)(\omega_p^2/c^2T^2)/[2\sqrt{\pi}\zeta^3\exp(-\zeta^2)]. \tag{15}$$

The Landau damping length equation (15) has a minimum at $\zeta = \sqrt{1{\cdot}5}$. Though the minimum is a false one due to the failure of the asymptotic expansion, $\zeta = 1{\cdot}22$ can be taken as the value for maximum Landau damping because the wave hardly propagates for smaller values of ζ. Using $\zeta = 1{\cdot}22$, one finds that Landau damping dominates for densities below about $10^{14}\,\mathrm{cm}^{-3}$ at 30 MHz and 3 eV.

To see the scalings more clearly, we change from mks to more convenient units. We now measure density in units of $10^{14}\,\mathrm{cm}^{-3}$ ($n_{14} = n/10^{20}$), frequency in MHz ($f_6 = f/10^6$), temperature T_e in eV, magnetic field in kG ($B_3 = 10B$), r and a in cm, and α, k, and T in cm^{-1}. We define the energy of resonant particles E_r to be $m(\omega/k)^2/2$, or in

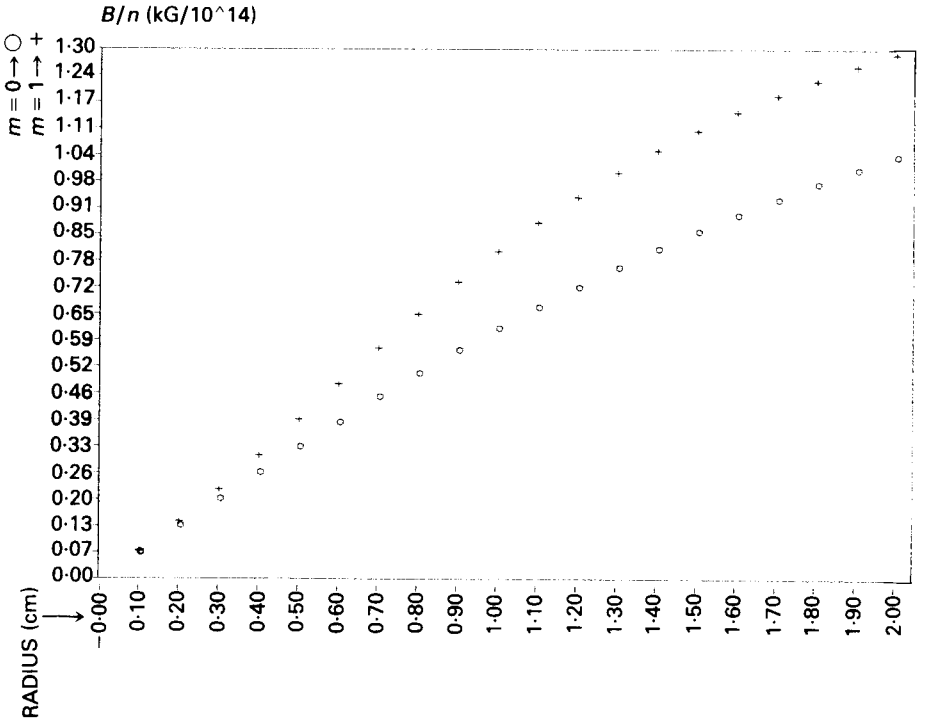

FIGURE 1. Calculated value of B_3/n_{14} vs. tube radius a (in cm) for $T_e = 3$ eV, and for the $m = 0$ (○) and $m = 1$ (+) modes.

the new units,

$$E_r\,(\text{eV}) = 0{\cdot}011 f_6^2/k^2. \tag{16}$$

Equations (5), (14), and (15) can then be written

$$B_3/n_{14} = 1{\cdot}20\sqrt{E_r}/\alpha \tag{17}$$

$$L_c = 15{\cdot}3(f_6/T^2k)(T_e^{\frac{3}{2}}/Z \ln \Lambda) \tag{18}$$

$$L_{LD} = 100(n_{14}/T^2k)\exp(\zeta^2)/\zeta^3. \tag{19}$$

Since $\alpha \simeq T \simeq 3{\cdot}83/a$ for the lowest radial mode, equation (17) shows that n_0/B_0 is a constant varying as $1/a$ and the chosen value of k/f. For each value of k, one finds T (and thus α) from equation (11) for the $m = 0$ mode, and from solution of equation (12) for the $m = 1$ mode. Further specifying f and n allows one to compute the damping lengths L_c and L_{LD} and the combined length $L_d = (1/L_c + 1/L_{LD})^{-1}$. The value of k can be chosen so that E_r is the energy of ionizing electrons or so that $\zeta = 1{\cdot}22$ for efficient wave absorption. Figure 1 shows the dispersion relation, B_3/n_{14} vs. a, for the $m = 0, 1$ modes and for $T_e = 3$ eV; equation (12) was solved by iteration.

3. Apparatus

Figure 2 shows a schematic of the apparatus. The vacuum chamber is a 40-cm long quartz tube with 1-cm inside radius. The base pressure is 2×10^{-5} torr, and the fill gas is 1–10 mTorr of argon. The magnetic field is produced by four coils, each about 10 cm long and 4·8 or 2·2 cm in radius. The smaller coils are mirror coils at the ends

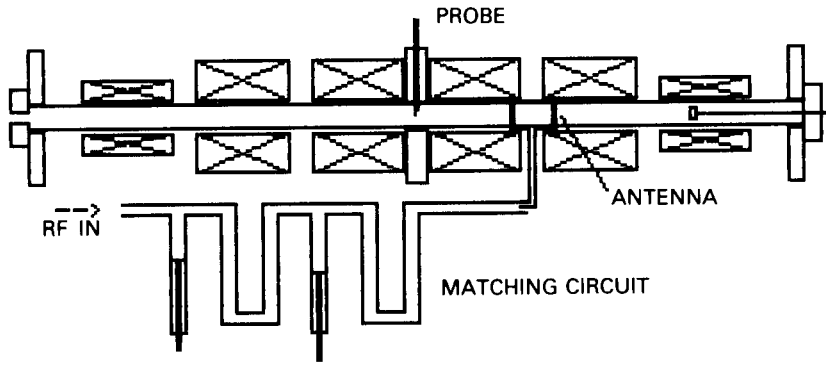

FIGURE 2. Schematic of the apparatus.

controlled by a separate power supply. Although the plasma is too collisional to benefit from mirror confinement, the end coils extend the region of field uniformity (±7%) to over 50 cm. Figure 3 shows the field shape and location of the coils and antenna. Probes, gas feed, and pressure sensor are placed in the 3-cm center gap. Maximum field is about 1 kG.

The rf system consists of a 750-W, 30-MHz amplifier driven by an oscillator and preamplifier. The external antenna is of the Nagoya Type III design (Watari *et al.* 1978), 4 cm long, containing a half wavelength. The imposed phase velocity resonates with electrons of about the ionization threshold energy of 15·7 eV. This type of antenna couples strongly to the plasma by inducing an internal electrostatic field (Chen 1981). The mode pattern of equations (6) and (7) shows that the wave electric field is

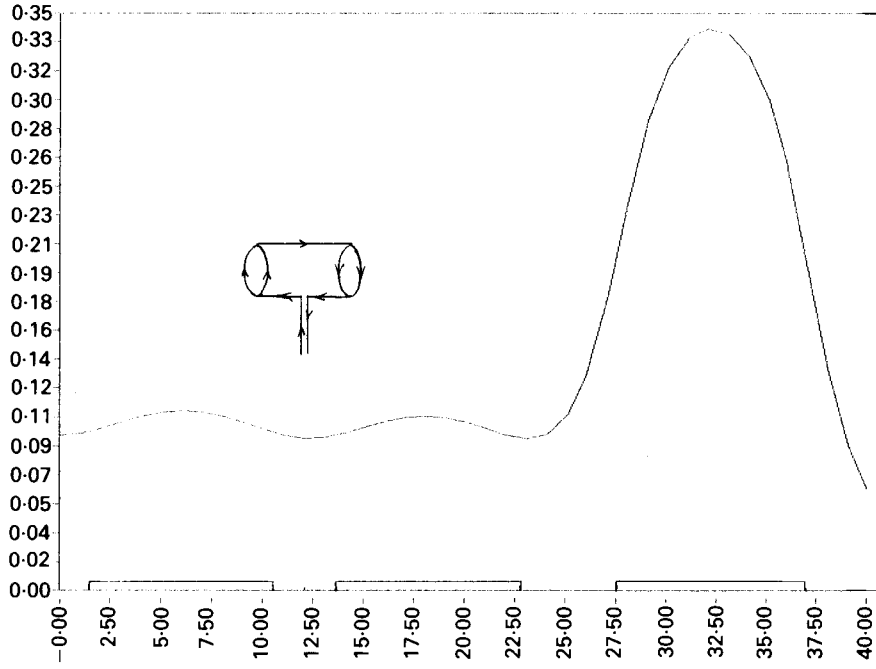

FIGURE 3. Calculated magnetic field profile vs. distance from the mid-plane, in cm. The locations of and lengths of the coils and of the rf antenna are shown to scale.

right-hand circularly polarized in the core of the plasma. Thus, only half the power in our plane-polarized antenna is used directly to excite the wave. The antenna is located between the second and third coils, half way between the midplane and the end of the uniform-field region.

Power is coupled to the antenna through a double-stub, quarter-wavelength matching circuit made from low-loss, 2-cm diameter rigid coaxial line. This is the most critical part of the apparatus. By tuning the two trombone legs, it is possible, when the wave is resonantly excited, to reduce the reflected power to less than 2%. More consistent results, however, are obtained when the tuning is slightly off the optimum, so that the system is less sensitive to slight variations in the plasma.

To avoid excessive heating of the matching circuit, we operated in a long-pulse mode. The magnetic field is on for 200 msec every few seconds, and the rf for 100 to 300 msec. The magnetic field can also be swept on a 100 msec timescale by slowing its rise and fall with large capacitors. For diagnostics we used a simple Langmuir probe 0·5 mm in diameter and 1·5 mm long, with a 1·5-mm diameter insulator, located at the midplane.

4. Observations

The plasma is observed to be brightest directly under the antenna, and the intensity reaches the far end of the tube only at the lowest pressures (1–2 mTorr); it barely reaches the midplane at the highest pressures (7–10 mTorr). These observations are consistent with estimates of radial diffusion. For magnetic fields of 100–1000 G, the electrons are highly magnetized, but the ions hardly at all. Radial diffusion of ions is reduced by the ambipolar field to the same rate as for electrons, which collide with ions more than with neutrals. The parallel diffusion of ions, however, is controlled by the

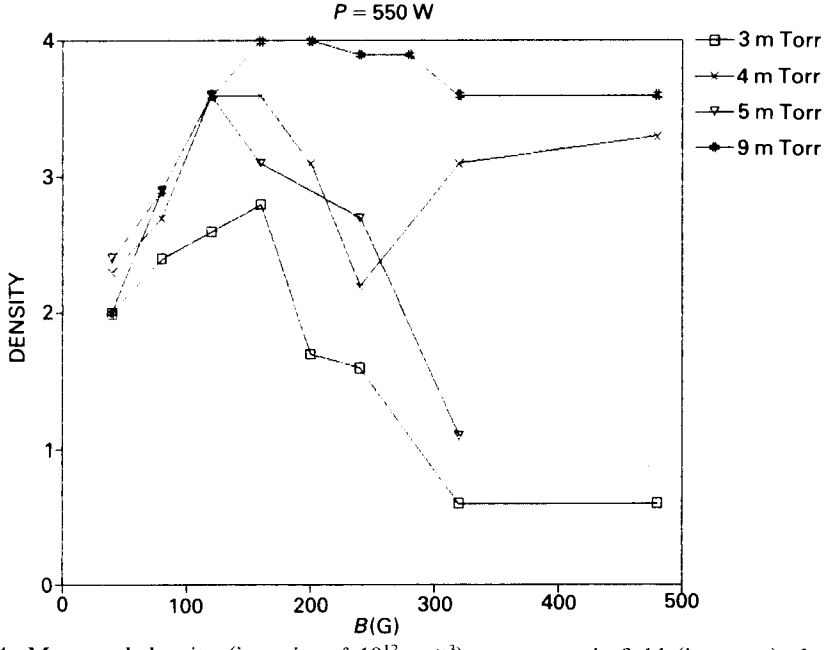

FIGURE 4. Measured density (in units of 10^{12} cm^{-3}) vs. magnetic field (in gauss), for rf power $P = 550$ W and pressures of 3 (□), 4 (×), 5 (▽), and 9 (#) mTorr. Large densities above 300 G cannot be maintained because of relaxation oscillations (see text).

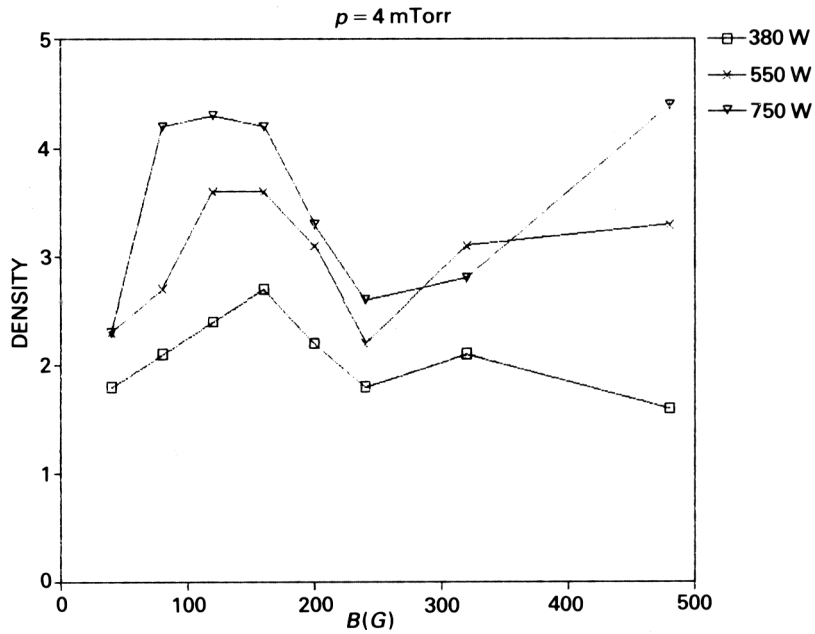

FIGURE 5. Measured density (in units of $10^{12}\,\mathrm{cm}^{-3}$) vs. magnetic field (in gauss), for 4 mTorr pressure and rf powers of 380 (□), 550 (×), and 750 (▽) W. As in figure 4, the densities above 300 G cannot be realized.

charge-exchange rate with neutrals. At typical operating conditions of $p \simeq 5$ mTorr, $n \simeq 5 \times 10^{12}\,\mathrm{cm}^{-3}$, and $B \simeq 100$ G, ions are lost radially before they reach the other end. The helicon wave is damped in about the same distance.

Figure 4 shows plasma density vs. magnetic field for various pressures at constant rf power, and figure 5 shows the same at constant pressure for various rf powers. In both cases there is a peak in density at an optimum field, indicating a wave resonance. The peak density achievable is limited by the available rf power, since the diffusive losses must be balanced by ionization. At the density limit, there is a value of B which

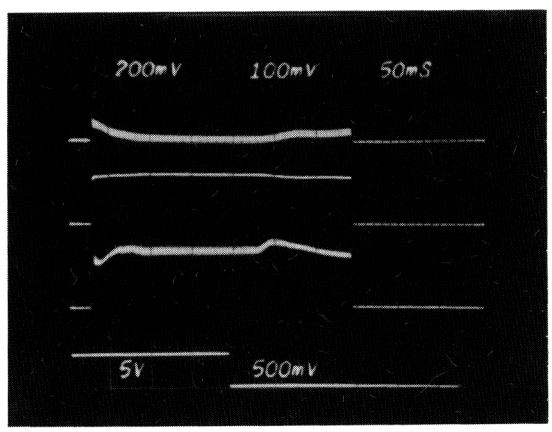

FIGURE 6. Oscillogram of a typical pulse: (A) reflected rf power, with gain 5 times that of (B); (B) incident rf power; (C) probe signal (saturation ion current); (D) B-field gate. Sweep speed: 50 msec/div. The field rises and decays with a 100-msec time constant but cannot be shown because of rf pickup.

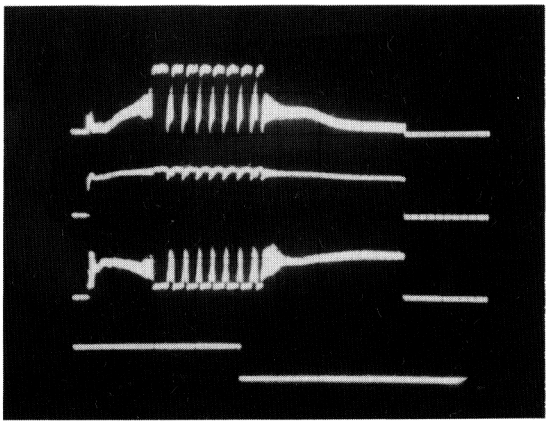

FIGURE 7. Oscillogram of a pulse at high field showing relaxation oscillations. Traces are the same as in figure 6.

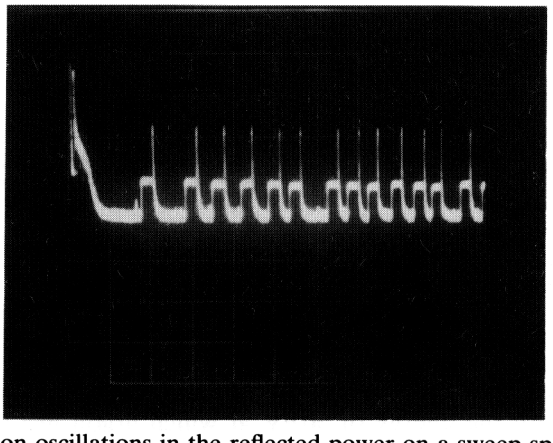

FIGURE 8. Relaxation oscillations in the reflected power on a sweep speed of 5 msec/div.

satisfies the dispersion relation, equation (17), giving rise to the peak. If the ionization were non-resonant, the density would rise monotonically with B, or, at worst, stay constant.

The magnetic field resonance can easily be seen in a single discharge in which the field is swept. In figure 6, B has been set at a value above its optimum value, and one sees that the density increases after the gate, during the decay of the field. The reflected power also decreases when the wave is excited. When B is set to even higher values, relaxation oscillations occur between states of non-resonant rf heating and helicon-wave heating, as illustrated in figure 7. The reflected power is seen to increase during non-resonant absorption. In figure 8, an expansion of the reflected power trace shows the three states of breakdown, wave generation, and non-resonant absorption.

5. Discussion

From the peaks found in figures 4 and 5, one can calculate a value of B_3/n_{14}. These average to a value of 4·5. This is plotted in figure 9 on a graph of the calculated value of this ratio for various resonant energies E_r. Also shown is the value of E_r corresponding to the fundamental mode of the antenna ($m = 1$, $k = 2\pi/8\,\mathrm{cm}^{-1}$). It is

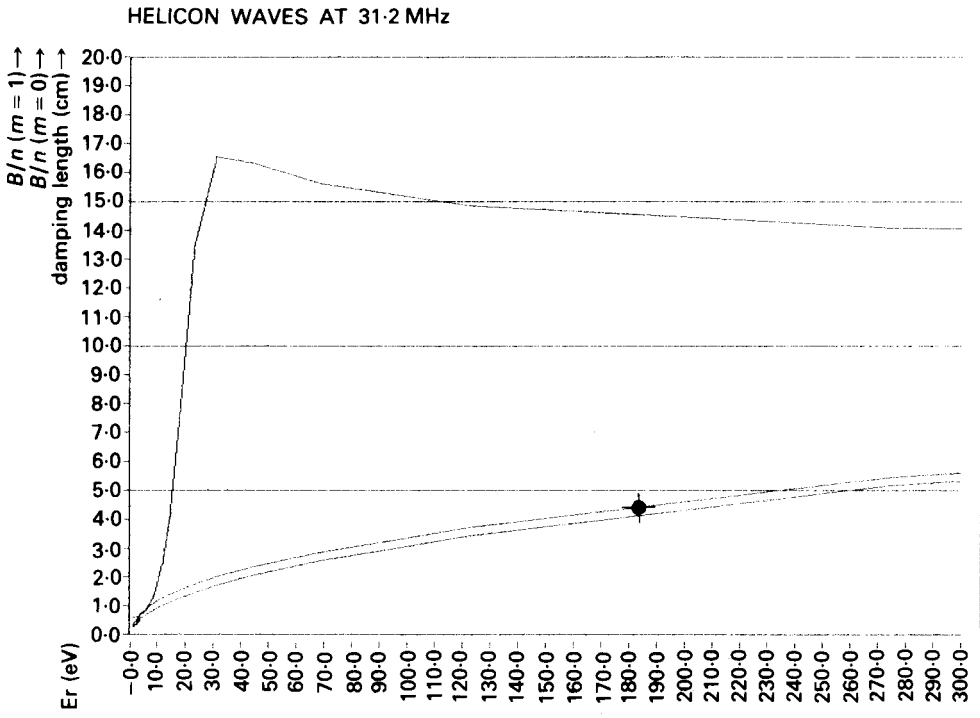

FIGURE 9. Calculated values (curves) of B_3/n_{14} vs. resonant particle energy (eV) for the $m = 0$ and 1 modes (lowest and middle curves, respectively). The point is the measured value. The upper curve is the computed damping length in cm.

seen that the measured value of B/n corresponds to an electron energy of about 200 eV, compared with the energy of 50 eV at which argon has its highest ionization cross section. The disagreement in the optimum phase velocity is only a factor of 2.

There are three parts to the operation of rf plasma sources: (1) antenna coupling, (2) wave dispersion, and (3) discharge physics. (1) In Nagoya Type III antennas, the plasma amplifies the applied electric field by a factor $(k_\perp/k_\parallel)^2$ (Chen 1981). The present antenna is rather short for its diameter; better coupling could be achieved by using a longer antenna and lowering the frequency to keep the phase velocity at the right value. (2) Our preliminary results give encouraging, if not exact, verification of helicon wave theory. Since n/B scales as $1/a$, one hopes, with sufficient rf power, to achieve densities high enough to be of use in accelerator applications by simply reducing the radius. For densities above $10^{14}\,\mathrm{cm}^{-3}$, the waves would be damped by collisions, but the Landau effect can still be used to accelerate the ionizing electrons. The magnetic fields and rf powers required are modest compared with those in other methods. (3) The main problem in discharge physics is plasma confinement. For the fully ionized plasmas which we hope to get, the diffusion coefficient $D_\perp$ varies as n/B^2. Thus, the particle loss rate $-D_\perp \nabla n$ depends only on n^2/B^2 (in addition to T_e and geometrical factors). Since $n/B \propto 1/a$ for helicon waves, large n cannot be attained simply by increasing B. The confinement time $\tau \simeq a^2/D_\perp$ is proportional to

$$\tau \propto a^2B^2/n = a^2n(B/n)^2 \propto na^4. \tag{20}$$

The required rf power per unit length of plasma varies as the number of particles

divided by the average confinement time; thus

$$P \propto na^2/\tau \propto na^2(n/a^2B^2) = n^2/B^2 \propto 1/a^2. \tag{21}$$

Because of increased diffusion, reducing the diameter to achieve higher densities comes at the expense of rf power. This is the reason, we believe, that Boswell *et al.* (1982, 1984), using larger tubes, were able to generate higher density plasmas with comparable rf power.

In summary, the production of higher densities requires high magnetic fields and small diameters. The latter shortens the confinement time and thus requires more power. However, the pulses can be very short in accelerator applications. The rf frequency matters only in the antenna coupling. The dependence on T_e is weak.

In this experiment, the frequency was well above the lower hybrid frequency of argon, but for lighter gases the theory must be modified to include ion effects. In future work, we hope to vary the gas, frequency, and antenna design. New probe techniques will have to be developed to study the mode structure of the rf field and measure dc quantities in its presence.

6. Acknowledgments

The author is greatly indebted to T. Shoji of the Nagoya Institute of Plasma Physics for help in the construction of the equipment, especially the design of the matching network, and for pointing out an error in the original theory (Chen 1985). C. Decker helped with the measurements. This work was supported by the National Science Foundation, Grant ECS 87-12089.

REFERENCES

Boswell, R. *et al.* 1982 *Phys. Letters* **91A,** 163.

Boswell, R. W. 1984 *Plasma Physics and Controlled Fusion* **26,** 1147.

Chen, F. F. 1981 TRW Report Task II-3552 (unpublished).

Chen, F. F. 1984 Introduction to Plasma Physics and Controlled Fusion, 2nd ed. (Plenum, New York), p. 270.

Chen, F. F. 1985 Australian National University Report ANU-PRL-IR 85/12 (unpublished).

Chen, F. F. 1989 *Physics of Laser Plasma,* A. Rubenchik and S. Witkowski, eds., in *Handbook of Plasma Physics,* R. Z. Sagdeev and M. N. Rosenbluth, eds. (North Holland, Amsterdam) Vol. 4, to be published.

Watari, T. *et al.* 1978 *Phys. Fluids* **21,** 2076.